

Power Flow Control with A Single Stage Grid Connected PV Mechanism with A Multilevel Inverter

U. K. Sinha

Department of Electrical Engineering, NIT Jamshedpur, India

ABSTRACT

There is potential to feed excess electricity to the grid for more efficient and cost-effective power utilization when solar PV arrays are installed widely in comparison to other renewable power output. The primary objective of this article is to use a multilevel inverter to operate autonomously regulate the active and reactive power flow. A vector control system that rotates synchronously with the grid frequency has been devised in both direct and quadrature reference frames. Two current control loops have been implemented to control the current delivered to the grid so that it will have low total harmonic distortion and is in phase with the grid voltage. To run the inverter at a suitable DC link voltage which corresponds to maximum power-which is established by the MPPT algorithm, a DC voltage control loop has also been implemented. Inverters that are connected to the grid are commonly utilized to enhance dispersed generation and power eminence.

Keywords: PV system, MPPT algorithm, Multilevel Inverter, Utility grid.

1. Introduction

There are possibilities to feed excess electricity to the grid for more efficient and cost-effective power consumption when solar PV arrays are installed widely as compared to other renewable power generating [1]. The self-regulation of the actual and reactive power flow of a single-stage grid-connected photovoltaic arrangement with a multilevel inverter is presented in this study. A vector control system that rotates synchronously with the grid frequency has been devised in both direct and quadrature reference frames. In order to ensure that the current injected into the grid is in phase with the grid voltage and has negligible total harmonic distortion, two current control loops, one for the d-axis and one for the q-axis, have been implemented. In addition, a DC voltage control loop has been built to operate the inverter at the intended DC bus voltage, which is the DC voltage that corresponds to maximum power and is established by the MPPT algorithm. Grid coupled inverters are widely used in various fields of power quality and distributed generation. The system mentioned previously takes advantage of a three-phase, three-level, Diode clamped multilevel inverter to increase the current pushed into the grid. It is essential that you guarantee that, in every application, the switching frequency ripple introduced into the grid by the grid-associated inverter stays within the parameters given by the grid standards. Furthermore, frequent grid disruptions such as voltage swells and sags are anticipated for the grid-connected inverter [2, 3]. Grid-connected inverters are projected to have excellent control performance since this ensures that it will operate throughout these disturbances and Neural-Network-Based MPPT Control of a Stand-Alone Hybrid Power

Generation System [4,18]. Additionally, grid-connected inverters' involvement in high power applications has limited their power handling capacities to a few megawatts today. The input DC bus voltage should be fixed at the maximum power point voltage (MPPV), which is the voltage at which the maximum real power is delivered from the PV source to the load, to obtain the desired inverter output voltage. Consequently, the dc link voltage has been managed using a voltage control.

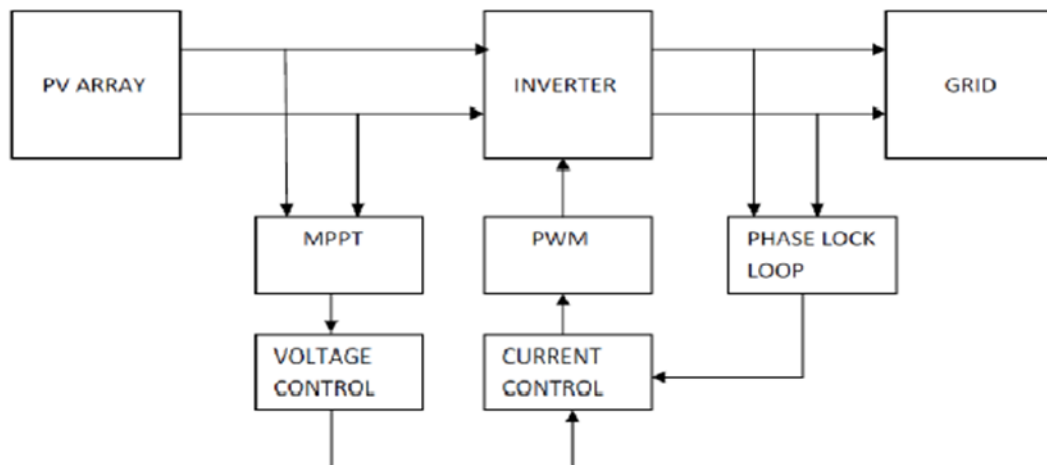


Fig. 1: Block diagram of single stage grid connected PV Array

To determine the MPPV, incremental conductance has been employed. For grid-connected PV systems, single-stage setups provide an integrated explanation of all the functions, including MPPT, inversion, and boosting (if required).

2. Control Scheme

In grid connected system there are several parameters that need to be controlled, among them fore most important are grid frequency and grid voltage. Also, in 3phase system, it requires separate control for all the three phases. This will result in a less effective and complex system. To ensure that the voltage space vector always stays constant regarding the d-q reference frame, it is therefore always preferable to carry out all control mechanisms in the two-phase DC frame [6, 7]. Therefore, a single, straightforward DC control system can solve the complexity issue of three-phase control.

2.1 Maximum Power Point Tracking

MPPT techniques are used in PV systems to take advantage of the output power of the PV array by continuously monitoring the MPPT, which is dependent on the temperature of the panel and on irradiation conditions [8, 9, 19, 20, 21]. We have tracked the MPPT of this PV array using the incremental conductance approach, one of many different tracking techniques. The PV array in the model below includes 29 series modules per string. At a temperature of 25 degrees Celsius and an irradiation of 1000 W/m², each module's MPP voltage is 29 V [10,11].

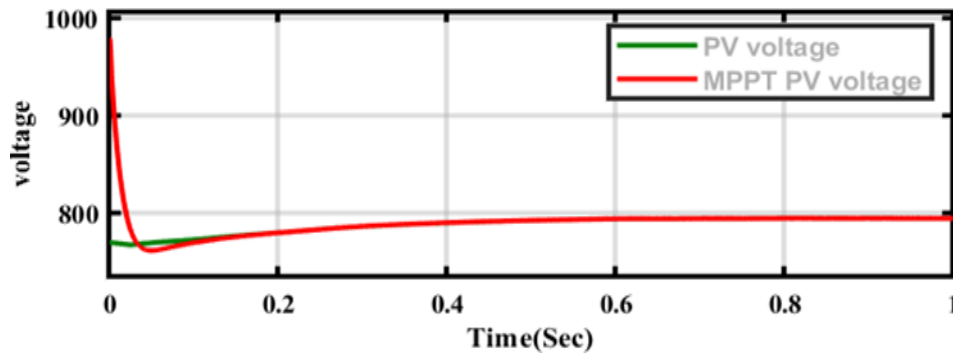


Fig. 2: MATLAB simulation graph of MPPT

3. PLL-based grid synchronization

The Phase Locked Loop (PLL) is employed to match the input phase with the local signal phase. The Phase Locked Loop is used to synchronize the output of the grid linked converter associated with the grid in a three-phase grid setup. PLL gives information on the grid voltage's frequency, phase, and amplitude. Grid-coupled power converters require PLL for closed-loop control and monitoring [11]. The Phase Locked Loop generates unit vectors that are utilized to generate reference signals for the closed loop rotating reference frame regulation of grid allied inverters.

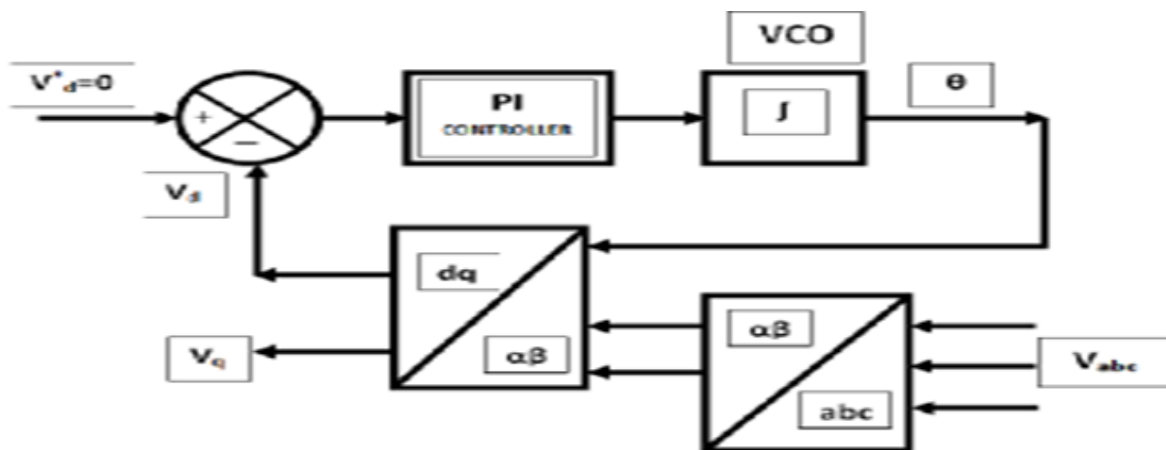


Fig.3: Schematic representation of PLL block

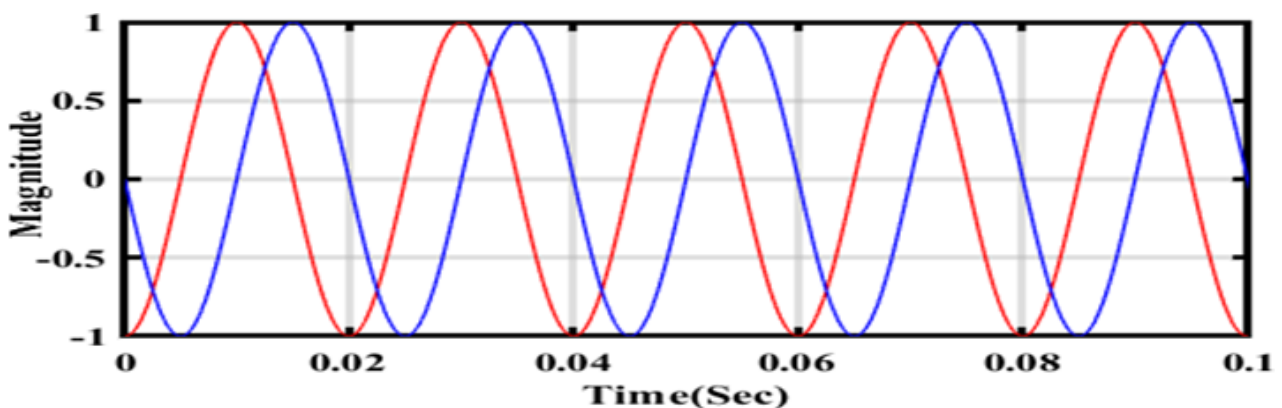


Fig. 4: Negative Feedback Current Control Loop

3.1 Current control

To achieve optimal power output and desired power quality, the grid current must be regulated. Figure 4 shows the graphic depiction of the current regulator loop. We have two current control loops because the d-q reference frame has two components for grid current: I_d , which is responsible for reactive power transfer, and I_q , which is responsible for real power transfer.

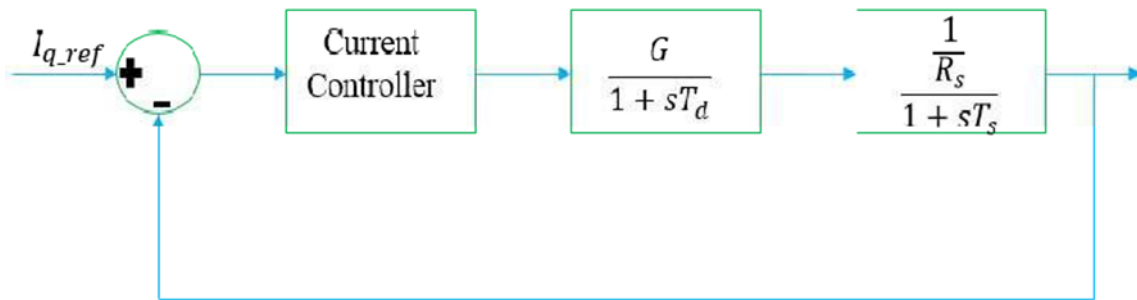


Fig.5: Negative feedback Current control loop

Reactive component must be zero for the converter to operate effectively at zero power factor angle, which means that the grid current injected is at unity power factor with respect to grid voltage. PI-controllers are provided with the error for both the direct and quadrature axes when the reference values of I_d and I_q , which are produced by the MPPT block, are compared with the feedback variables [12]. Current controller transfer function $G_c(s)$ from the current regulation loop can be written as follows:

$$G_c(s) = \left[\frac{G}{(1+R_s)} \right] / \left[(1+sT_s) \right] \tag{1}$$

Where G is the gain of inverter model, $G = V_{dc}/V_c$

Where, V_{dc} is the DC bus voltage and V_c is peak amplitude voltage of the carrier wave, T_s is the delay time, T_s is the inductor time-constant, where R_s and L_s is its resistance and inductance, C is the input capacitance and K is the sensor gain. The current regulator parameters K_p and K_i can be obtained by comparing equation (1) with the PI controller transfer function i.e., $K_i/s + K_p$.

3.2 DC voltage Control

In accordance to regulate the DC bus voltage at MPP voltage, this voltage regulation loop allotted. To maintain the DC voltage at a constant value, the error between the reference DC bus voltage that is the tracked MPPV, and the feedback DC bus voltage is delivered via a PI-type compensator. The outcome of the compensator maintains the reference for active component of current that is the quadrature axis current. The implementation of the regulation scheme for the system, the inverter should be mathematically modelled.

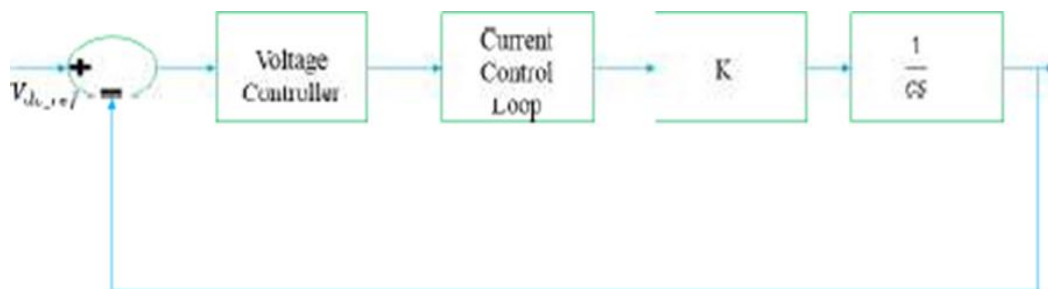


Fig.6: Negative feedback Voltage control loop

From the above control loop, the voltage controller parameter can be found. Let $G_v(s)$ is voltage controller transfer function. Thus, it is,

$$G_v(s) = G(s)(k/sC) \tag{2}$$

The PI-controller parameters that are K_p and K_i (proportional and integral constant) for the voltage control loop can be obtained from the current control loop and the input capacitance along with the sensor [13] gain as shown in equation (2).

3.3 Modelling of Grid Connected VSI

For a 3-phase grid connected inverter, the single-phase diagram is shown below,

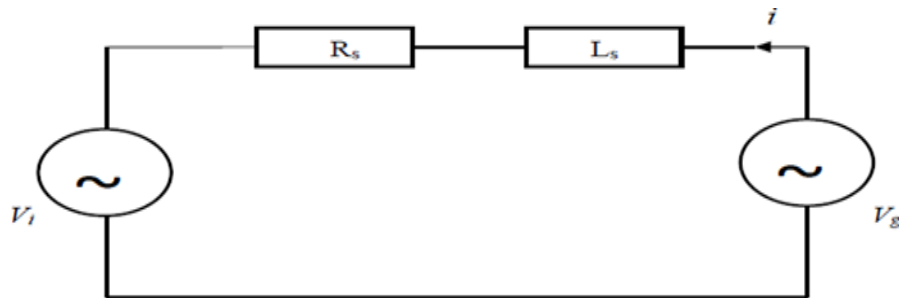


Fig. 7: 3-phase Grid Connector Inverter

$$V_g = V_i + iR_s + L_s \frac{di}{dt} \tag{3}$$

$$\text{Let, } V_g - V_i = D$$

$$V_g = V_{ga}, V_{gb}, V_{gc}$$

$$V_i = V_{ia}, V_{ib}, V_{ic}$$

$$i = i_a + i_b + i_c$$

$$\frac{di}{dt} = \frac{di_a}{dt}, \frac{di_b}{dt}, \frac{di_c}{dt}$$

$$\frac{di}{dt} = (D/L_s) - iR_s/L_s$$

Now, current equation of d-q reference frame in terms of α - β reference frame considering $\theta = 90^\circ + \omega t$,

$$i_d = i_\beta \cos \omega t - i_\alpha \sin \omega t \tag{4}$$

$$i_q = -(i_\beta \sin \omega t + i_\alpha \cos \omega t) \tag{5}$$

Differentiating equations (4) and (5) and substituting di_α/dt and di_β/dt from equation (1), we get,

$$D i_d / dt = (D/L_s) - i_d (R_s/L_s) + \omega i_q \tag{6}$$

$$D i_q / dt = (D/L_s) - i_q (R_s/L_s) + \omega i_d \tag{7}$$

$$V_{gd} = V_{id} + L_s (di_q/dt) + R_s i_d - \omega L_s i_q \tag{8}$$

$$V_{gq} = V_{iq} + L_s (di_d/dt) + R_s i_q + \omega L_s i_d$$

(9)

For reactive power component to be zero i.e., $V_{gd} = 0$, hence from Equation (8), we get the Equation (10) as below:

$$V_{id} + L_s (di_q/dt) + R_s i_d - \omega L_s i_q = 0 \tag{10}$$

Thus, for d-q axis component of voltage has cross coupling with each other. So, in mandate to have independent regulation of real and reactive power components. We must add a feed forward block which cancels out the effect of cross coupling [14].

$$V_{dcc} = G \omega i_q \tag{11}$$

$$V_{qcc} = G(V - \omega L_s i_d) \tag{12}$$

The equation of real and reactive power transmitted in direct and quadrature reference frame after implementing this decoupled power flow control is given as below:

The real power,

$$P = \frac{2(V_d i_d + V_q i_q)}{3}$$

Or, $P = 0.67 V_q i_q$ (13)

The reactive power,

$$Q = \frac{2(V_d i_q + V_q i_d)}{3}$$

Or, $Q = 0$ (14)

3-phase grid connected inverter of a vector control scheme is presented in Figure 7. The different blocks are used for control calculations in d-q reference frame. Again, these variables are transformed in a-b-c reference frame after performing all calculations and feed it to PWM block for the three-level inverter switches. The complete system from PV array to grid can be modelled as shown below [15, 16 17].

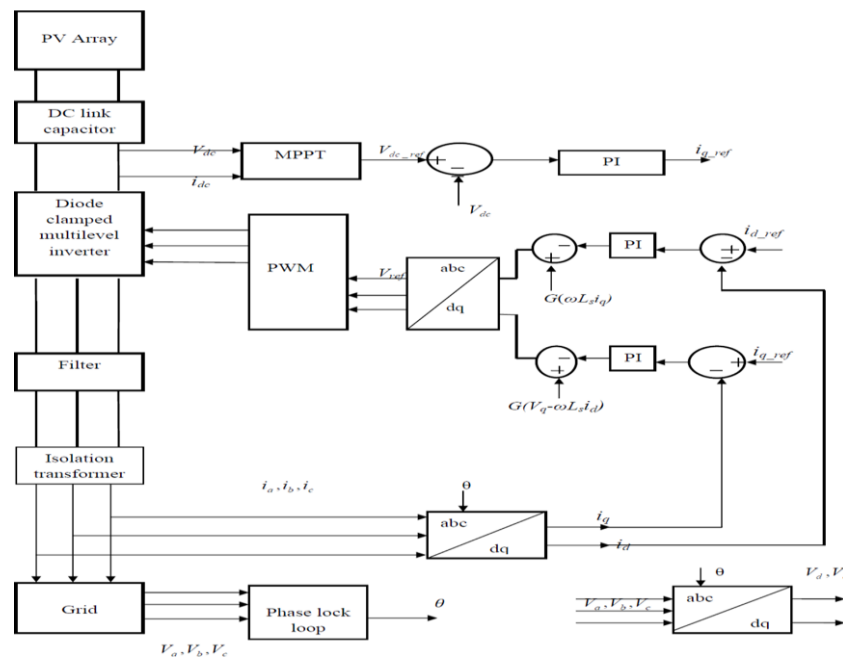
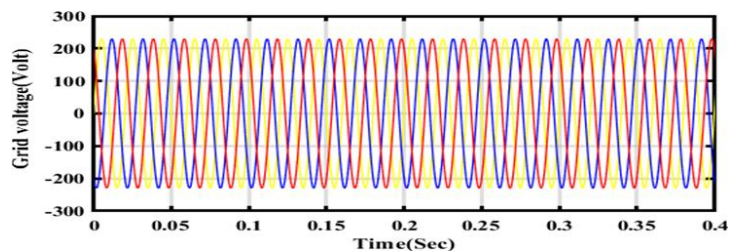


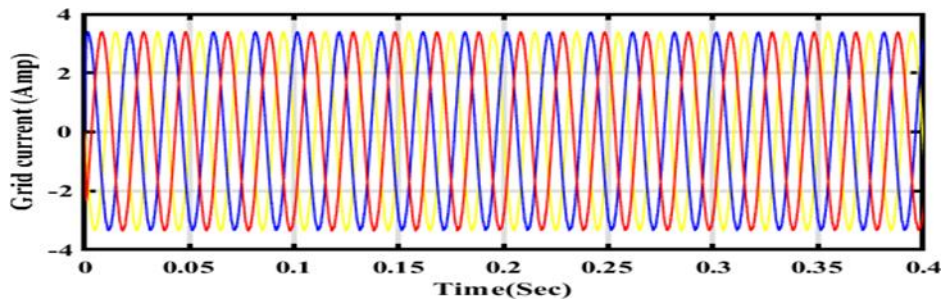
Fig.8: Control Scheme from PV to Grid

3.4 Simulation Results and Discussions

The results obtained by the simulation have been presented for different parameters from Fig. 8 to Fig. 11 as below:

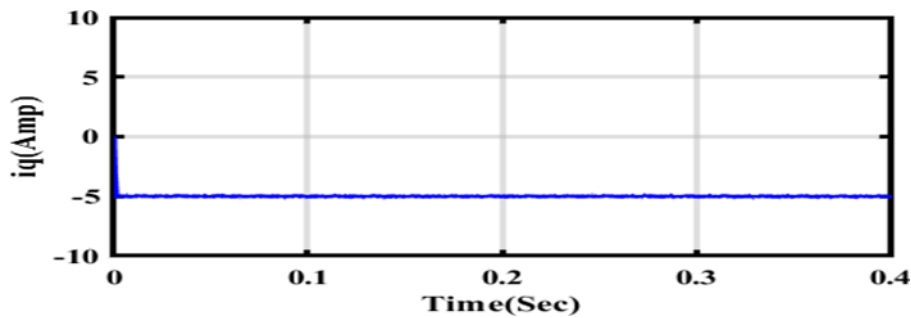


8(a)

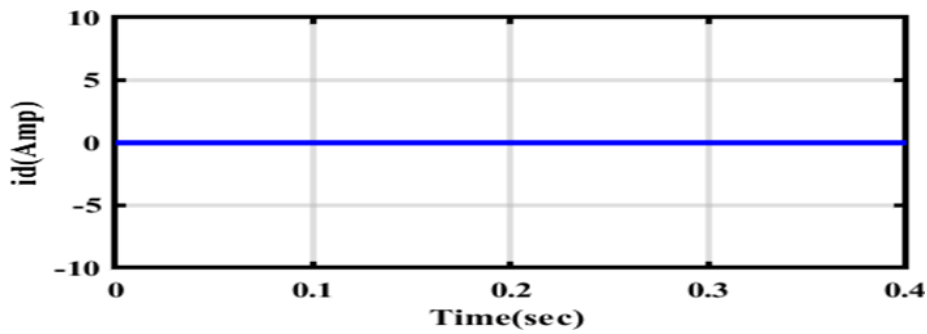


8(b)

Fig. 8 (a) Grid voltage (b) Grid current at $i_{q,ref}=-5$, $i_{d,ref}=0$, $V_{dc}=300V$

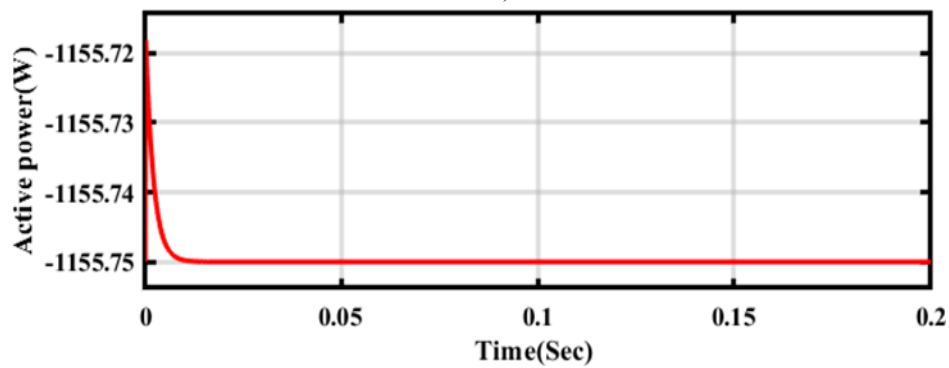


9(a)

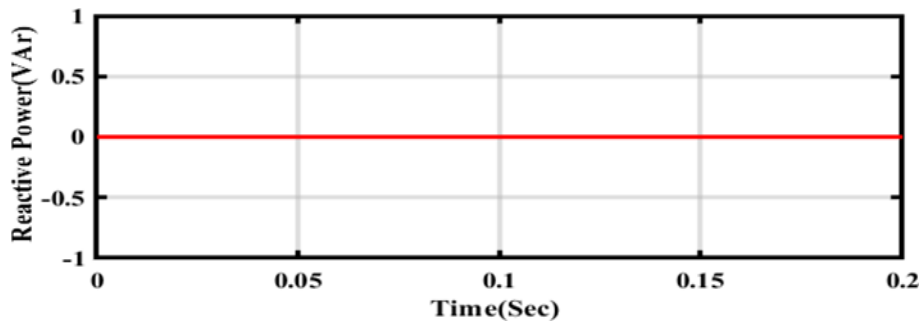


9(b)

Fig. 9: (a) quadrature axis grid current (b) direct axis grid current at $i_{q,ref}=-5$, $i_{d,ref}=0$



10(a)



10(b)

Fig.10: (a) Active power (b) Reactive power at $i_{q,ref} = -5$, $i_{d,ref} = 0$ and $V_{dc} = 300V$

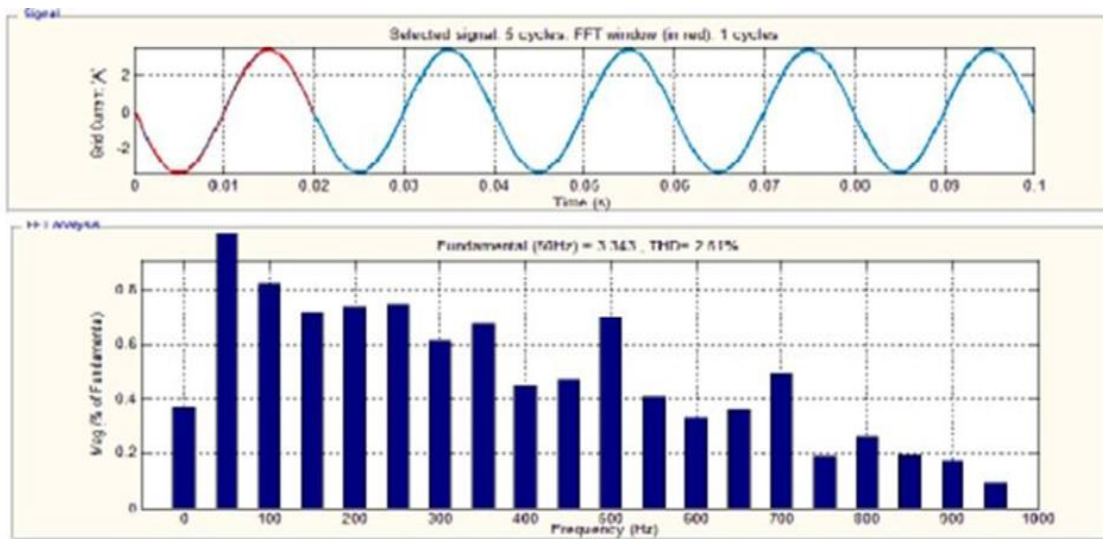


Fig. 11. THD analysis of grid current at $i_{q,ref} = -5$, $i_{d,ref} = 0$ and $V_{dc} = 300V$

4. CONCLUSION

The use of MATLAB/Simulink, the suggested control system connected to a three-phase, three-level diode clamped inverter has demonstrated the effectiveness of the applied vector control approach for the decoupling management of real-life and the reactive power flow strategy from inverter end to grid end. Throughout, the DC bus's input voltage is fixed at 300V. Ten kHz is the switching frequency, and each phase is filtered by a 30mH inductance. The simulated data above makes it rather evident that the deliberate controller is achieving satisfactory outcomes. Grid currents rotate synchronously while maintaining references generated for current control loops, considering the feedback of the reference frame. With a DC-link voltage of 300V for active power transfer to the grid at $i_{q, ref} = -5$ and $i_{d, ref} = 0$ is achieved. By establishing appropriate references for the real and reactive current regulation loops in the synchronously rotating reference frame with zero power factor angle, autonomous control of both real and reactive power may be achieved. THD analysis of the grid current is shown in Figure 4.11, and the results are satisfactory. All these simulated results verify the effectiveness of the proposed regulating strategy. As a result, the feedback grid currents in the reference frame spinning synchronously keeping to the references established for the current control loops. Using, a DC link voltage of 300V for active power transfer to the grid at $i_{q, ref} = -5$ and $i_{d, ref} = 0$. By setting the appropriate references for the real and reactive current regulation loops in the synchronously rotating reference frame with zero power factor angle allows for the autonomous control of both real and reactive power. Figure 4.11 displays the grid current's THD analysis,

which gives acceptable findings. The performance of the suggested regulating technique is validated by all these simulated results.

REFERENCES

1. M. Galád, P. Špánik, "Design of Photovoltaic Solar Cell Model for Stand-alone Renewable System", 10th International Conference ELEKTRO 2014, pp. 285-288, 19–20 May 2014, ISBN 978-1-4799-3720-2.
2. Salama, A. Tabyaoui, M. Benchagra, "NPC Multilevel Photovoltaic Inverter with Nonlinear MPPT using Boost Converter", International Review of Automatic Control, vol. 10, no. 6, pp. 476-484, 2017.
3. J. S. Lai and F. Z. Peng, "Multilevel Converters – A New Breed of Power Converters," IEEE Transactions on Industry Applications, "vol. 32, pp. 509–517, June 1996.
4. C. D. Townsend, Y. Yu, G. Konstantinou, V. G. Agelidis, "Cascaded H-bridge multilevel PV topology for alleviation of per-phase power imbalances and reduction of second harmonic voltage ripple", IEEE Transactions on Power Electronics, vol. 31, no. 8, pp. 5574-5586, 2016.
5. Y. Shashi Kumar and Rajesh Gupta, "Maximum Power Point Tracking of Multiple Photovoltaic Arrays", Students Conference on Engineering and Systems (SCES), pp;1-6,2012.
6. W.C. Duesterhoeft, M.W. Schulz and E. Clarke, "Determination of Instantaneous Currents and Voltages by Means of Alpha, Beta, and Zero Components," Transactions of the American Institute of Electrical Engineers, vol. 70, no. 2, p. 1248–1255, July 1951.
7. J. M. Carrasco, L. G. Franquelo, J. T. Bialasiewicz, E. Galvan, R. P. Guisado, M.A. Prats, and N. Moreno-Alfonso, "Power-electronic systems for the grid integration of renewable energy sources: A survey," IEEE Transactions on Industrial Electronics, vol. 53, no. 4, pp. 1002-1016, 2006.
8. Yu. T. C., & Lin. Y. C., "A Study on Maximum Power Point Tracking Algorithms for Photovoltaic Systems." Luangwa University of Science and Technology, Dept. of Electrical Engineering, 2010.
9. A. Nicastrì and A. Nagliero, "Comparison and evaluation of the PLL techniques for the design of the grid-connected inverter systems," in IEEE International Symposium on Industrial Electronics (ISIE), 2010, pp. 3865- 3870, IEEE, 2010.
10. Sedo J and Kascak S, "Control of Single-Phase Grid Connected Inverter System," in IEEE 2016 ELEKTRO, 2016.
11. G. Walker, "Evaluating MPPT converter topologies using a MATLAB PV model," Journal of Electrical & Electronics Engineering, Australia, vol. 21, 2001.
12. Nicola Femia, Giovanni Spagnuolo, "Optimization of Perturb and Observe Maximum Power Point Tracking Method", IEEE transactions on Power Electronics Vol. 20, No. 4 July 2005.
13. A. Alexander, M. Thathan, "Modelling and analysis of modular multilevel converter for solar photovoltaic applications to improve power quality", IET Renewable Power Generation, vol. 9, no. 1, pp. 78-88, 2015.
14. O. Salama, A. Tabyaoui, M. Benchagra, "Analysis and comparison of Control on Power Converters in Photovoltaic Energy", Electrical and Information Technologies (ICEIT) IEEE International Conference on, pp. 1- 8, 2017.
15. D. Borgonovo, Modelling and Control of Three-Phase PWM Rectifier Using Park Transformation. Florianopolis, 2001. Dissertation of master's in electrical engineering - INEP, UFSC.
16. C. Cecati, A. Dell'Aquila, M. Liserre. A novel three-phase single-stage distributed power inverter. IEEE Transactions on Power Electronics, Volume 19, Issue 5, Sept. 2004 Page(s):1226 - 1233.

17. R. L. Carletti, L. C. G. Lopes, P. G. Barbosa, Active & Reactive Powers Control Scheme for a Grid-Connected Photovoltaic Generation System Based on VSI with Selective Harmonic Elimination. 8 Power Electronics Brazilian Conference, COBEP, Recife p. 129-134, 2005.
18. Whei-Min Lin, Member, IEEE, Chih-Ming Hong, and Chiung-Hsing Chen, “Neural-Network-Based MPPT Control of a Stand-Alone Hybrid Power Generation System” IEEE Transactions on Power Electronics, 2011, Vol. 26, No. 12.
19. Cherukuri SK, Rayapudi SR. Enhanced grey wolf optimizer based MPPT algorithm of PV system under partial shaded condition. Int J Renew Energy Dev. 2017;6(3):203. doi:10.14710/ijred.6.3.203-212
20. Peng B-R, Ho K-C, Liu Y-H. A novel and fast MPPT method suitable for both fast changing and partially shaded conditions. IEEE Trans Ind Electron. April 2018;65(4):3240–3251. doi:10.1109/TIE.2017.2736484
21. Wan Y, Mao M, Zhou L, et al. A novel nature-inspired maximum power point tracking (MPPT) controller based on SSA-GWO algorithm for partially shaded photovoltaic systems. Electronics (Basel). 2019;8(6):680. doi:10.3390/electronics8060680.